# Systemic Vascular Transduction by Capsid Mutant Adeno-Associated Virus After Intravenous Injection

Daniel M. Lipinski,[1,2,*] Chris A. Reid,[1] Sanford L. Boye,[1] James J. Peterson,[1] Xiaoping Qi,[3] Shannon E. Boye,[1] Michael E. Boulton,[3] and William W. Hauswirth[1]

[1]Department of Ophthalmology, College of Medicine, University of Florida, Gainesville, Florida; [2]Nuffield Laboratory of Ophthalmology, Department of Clinical Neuroscience, University of Oxford, Oxford, United Kingdom; [3]Department of Ophthalmology, Indiana University School of Medicine, Indiana University, Indianapolis, Indiana.

The ability to effectively deliver genetic material to vascular endothelial cells remains one of the greatest unmet challenges facing the development of gene therapies to prevent diseases with underlying vascular etiology, such as diabetes, atherosclerosis, and age-related macular degeneration. Herein, we assess the effectiveness of an rAAV2-based capsid mutant vector (Y272F, Y444F, Y500F, Y730F, T491V; termed QuadYF+TV) with strong endothelial cell tropism at transducing the vasculature after systemic administration. Intravenous injection of QuadYF+TV resulted in widespread transduction throughout the vasculature of several major organ systems, as assessed by *in vivo* bioluminescence imaging and postmortem histology. Robust transduction of lung tissue was observed in QuadYF+TV-injected mice, indicating a role for intravenous gene delivery in the treatment of chronic diseases presenting with pulmonary complications, such as $\alpha_1$-antitrypsin deficiency. The QuadYF+TV vector cross-reacted strongly with AAV2 neutralizing antibodies, however, indicating that a targeted delivery strategy may be required to maximize clinical translatability.

## INTRODUCTION

Dysfunction of vascular endothelial cells underlies the development and progression of several potentially life-threatening diseases, including diabetes mellitus,[1] hypertension,[2] atherosclerosis,[3] and coronary artery disease.[4,5] Although current drug-based therapies demonstrate that amelioration of vascular dysfunction can be successfully achieved through modulation of key endothelial cell-specific pathways,[6–16] treatment effects are invariably short-lived, requiring daily dose administration throughout a patient's lifetime. As a consequence, the ability to permanently modify endothelial cells through gene augmentation represents an exciting therapeutic avenue for the treatment of chronic vascular disease, potentially allowing long-term treatment to be achieved after a single intervention. However, previous efforts to target vascular endothelial cells *in vivo* through intravenous administration of native DNA[17] or of recombinant adeno-associated viral (rAAV)[18,19] or adenoviral vectors[20,21] have proven to be ineffectual, resulting in minimal vascular transduction and, frequently, acute systemic toxicity.[22,23]

Attempts have been made to improve on the native properties of rAAV vectors by introducing targeted mutations within the shared C-terminal domain of the structural proteins (VP1/VP2/VP3) that comprise the viral capsid (see Fig. 1A). Specifically, site-directed tyrosine-to-phenylalanine (Y–F) and threonine-to-valine (T–V) substitutions have been shown to effectively prevent phosphorylation and subsequent ubiquitin-mediated proteolysis of the capsid, resulting in substantially improved transduction efficiency and altered tropism in several tissues, including the eye,[24–26] brain,[27] and muscle.[28] Building on these studies, herein we evaluate a number of AAV serotype 2 (AAV2)-based vectors containing combinations of single-amino acid substitutions at specific sites throughout the shared C-terminal domain (Y272F, Y444F, T491V, Y500F, Y730F; see Fig. 1A) to determine their tropism for vascular endothelial cells when administered systemically.

*Correspondence: Dr. Daniel M. Lipinski, Department of Ophthalmology, College of Medicine, University of Florida, Gainesville, FL 32610. E-mail: dlipinski@ufl.edu



DOI: 10.1089/hum.2015.097

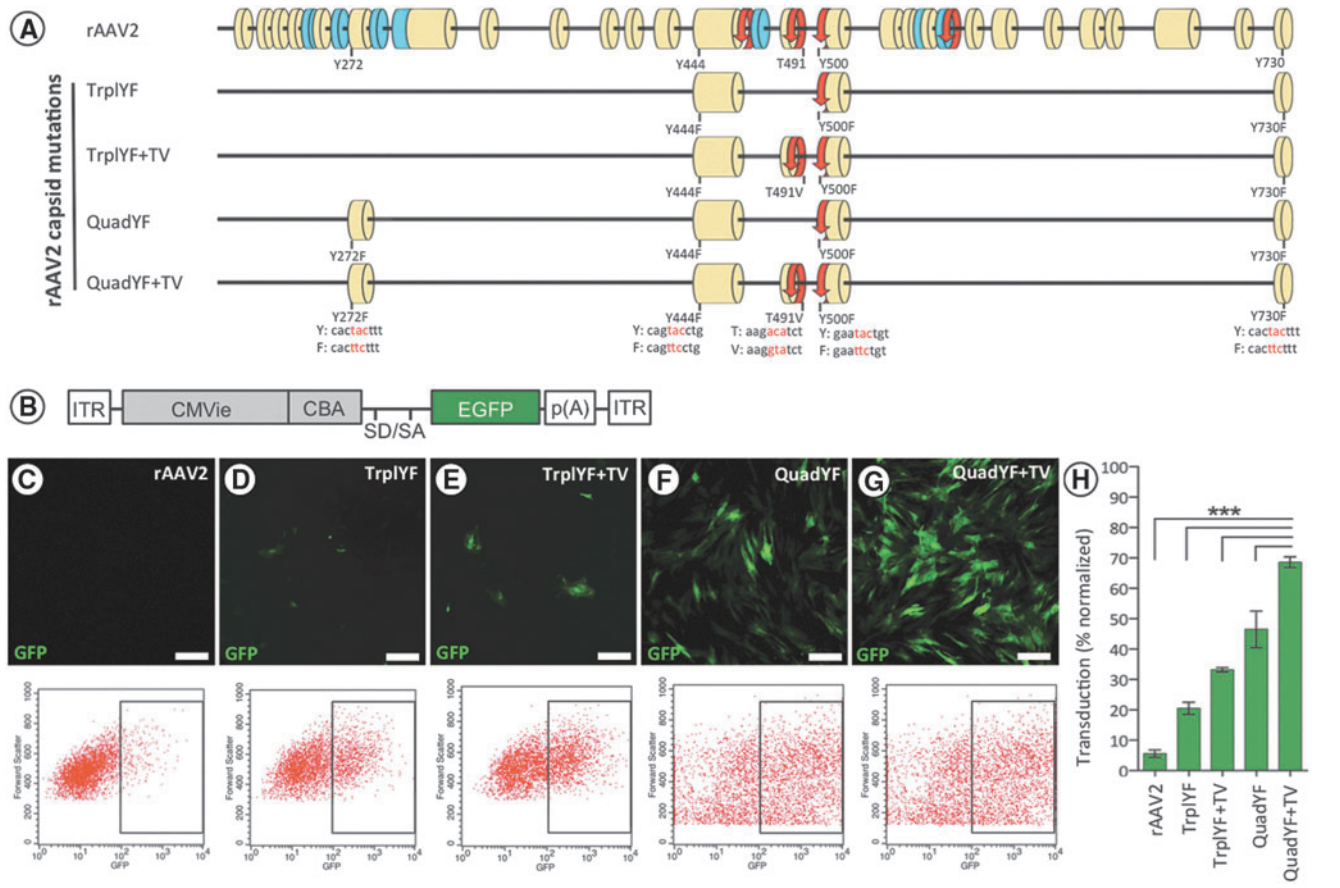


**Figure 1.** **(A)** Scale representation of the AAV2 capsid (Cap) protein shared VP1/VP2/VP3 C terminus highlighting the position of each capsid mutation relative to the major structural domains: yellow, $\beta$-strand; blue, $\alpha$-helix; red, turn. Amino acid substitutions of each capsid mutation are highlighted with corresponding genomic changes shown below in red. **(B)** Schematic representation of the ubiquitously expressing fluorescent reporter construct used for *in vitro* studies: ITR, inverted terminal repeat; CMVie, cytomegalovirus immediate-early enhancer; CBA, chicken $\beta$-actin promoter; SD/SA, splice donor/acceptor; EGFP, enhanced green fluorescent protein; p(A), polyadenylation signal. **(C–G)** Transduction of primary bovine endothelial cells (MOI of 100,000, all groups) demonstrates that efficiency increases additively with the numbers of capsid mutations present; the transduction efficiency of each vector was subsequently quantified by flow cytometry **(H)**. $n=3$–5 wells per vector, $^{***}p<0.001$, one-way ANOVA with Tukey post-hoc test. Scale bars, 20 $\mu$m.

## MATERIALS AND METHODS

### Animals

All animal experiments were performed in compliance with the Association for Research in Vision and Ophthalmology (ARVO) *Statement for the Use of Animals in Ophthalmic and Visual Research* and ARRIVE (Animal Research: Reporting of *in Vivo* Experiments) guidelines, and were conducted in accordance with an approved Institutional Animal Care and Use Committee protocol (principal investigator, D.M. Lipinski; protocol ID, 201308119). Eighteen juvenile (6–8 weeks of age) C57BL/6J or BALB/c mice were purchased from Jackson Laboratory (Bar Harbor, ME) and housed under standard 12:12 light/dark cycle conditions with food and water available *ad libitum*. Anesthesia was induced for all nonterminal procedures by a single intraperitoneal injection of ketamine (60 mg/kg body weight; Bioniche, Galway, Ireland) and xylazine (10 mg/kg body weight; Lloyd, Shenandoah, IA). Anesthesia was reversed after completion of the procedure by intraperitoneal injection of atipamezole hydrochloride (Antisedan, 5 mg/kg body weight; Orion Pharma, Espoo, Finland) and ophthalmic ointment (2.5% hypromellose; Akorn, Lake Forest, IL) applied to prevent corneal desiccation.

### Vector production

AAV vector preparations were produced by a double-plasmid cotransfection method, as described previously.[29] Briefly, one CellSTACK (Corning, Corning, NY) seeded with approximately $1\times10^9$ HEK-293 cells was cultured in Dulbecco's modified Eagle's medium (HyClone Laboratories, Logan, UT) containing 5% fetal bovine serum (FBS) and antibiotics (cDMEM). Transfection precipitation was established by mixing a 1:1 molar ratio of

rAAV vector plasmid DNA and serotype-specific *rep–cap* helper plasmid DNA with calcium phosphate ($CaPO_4$), which was subsequently added to 1100 ml of cDMEM, applied directly to the CellSTACK, and incubated for 60 hr at 37°C, 7% $CO_2$. The cells were harvested and lysed by multiple (three) freeze–thaw cycles, and the crude lysate was clarified by centrifugation. The resulting vector-containing supernatant was divided among four discontinuous iodixanol step gradients, which were centrifuged at 350,000 × *g* for 1 hr. After centrifugation, approximately 5 ml of the 60–40% step interface was removed from each gradient and pooled before column chromatography on a 5-ml HiTrap Q Sepharose (anion-exchange) column, using a Pharmacia ÄKTAFPLC system (GE Healthcare Life Sciences, Pittsburgh, PA). The vector was eluted from the column with 215 m*M* NaCl, pH 8.0, and the rAAV peak was collected. The vector-containing fraction was then concentrated by buffer exchange in Alcon balanced salt solution (BSS; Alcon, Fort Worth, TX) containing 0.014% Tween 20, using a Biomax 100K concentrator (Millipore, Billerica, MA). Vector was then titered for DNase-resistant vector genomes by real-time PCR relative to a standard.

### *In vitro* transduction assay

Bovine retinal endothelial cells were harvested by filtration as described previously[30] and plated in 4-chamber glass slides (Lab-Tek; Electron Microscopy Sciences, Hatfield, PA) at a density of $1 \times 10^4$ cells per well. After a 24-hr period to allow for adhesion cells were transduced by the addition into the medium of unmodified AAV2 or capsid mutant AAV2-based vectors packaging an enhanced green fluorescent protein (EGFP) reporter construct driven by a vascular endothelial cell-specific promoter (VECadherin; cadherin-5). All vectors were applied at a multiplicity of infection (MOI) of 100,000 and three replicates (wells) were performed for each. Three days were allowed for virus expression, after which cells were fixed in 4% paraformaldehyde (PFA), imaged with an Olympus IX70 inverted fluorescence microscope, and subsequently detached (1% trypsin–EDTA) for quantification by flow cytometry with a FACSCalibur (BD Biosciences, Sparks, MD) cell analyzer optimized for quantification of EGFP-positive cells gated by size and granularity.

### Neutralizing antibody assay

Neutralizing antibody experiments were carried out as described previously.[24,31] Briefly, unmodified AAV2 and QuadYF+T491V capsid mutant vector (AAV vector incorporating five [Y272F, Y444F, Y500F, Y730F, T491V] mutations) packaging a self-complementary mCherry (red fluorescent protein) reporter gene driven by a ubiquitously expressing promoter (small chicken $\beta$-actin) were preincubated at 37°C for 1 hr in 2-fold dilutions (1:40, 1:80, 1:160, and 1:320) of serum known to contain a high (seropositive) or low (seronegative) concentration of AAV2 neutralizing antibodies. After incubation, vector-containing serum samples were applied to ARPE-19 cells seeded in 96-well plates at an MOI of 5000 for 1 hr before the addition of 100 $\mu$l of DMEM containing 20% FBS. ARPE-19 cells were selected because of their permissiveness to transduction by most AAV vector serotypes, including unmodified rAAV2. All samples (conducted in triplicate) were incubated for 72 hr to allow for transgene expression, fixed in 4% PFA, and subsequently detached (1% trypsin–EDTA) for quantification by flow cytometry with a FACSCalibur cell analyzer (BD Biosciences) optimized for quantification of mCherry-positive cells gated by size and granularity.

### Vector injection

After induction of anesthesia each mouse was placed in a left lateral recumbent position and the right eye was partially prolapsed by applying gentle pressure medially and laterally with the fingers. Injections were performed by advancing a low-volume disposable syringe (AirTite Norm-Ject; Henke Sass Wolf, Tuttlingen, Germany) with attached 27-guage intermediate-bevel needle (Covidien, Mansfield, MA) at an acute angle through the medial canthus into the retro-orbital venous sinus. Viral vector suspended in a total volume of 200 $\mu$l of BSS was injected into the vasculature of each experimental animal by slow manual perfusion. Any animals showing evidence of substantial reflux or bleeding were immediately killed and excluded from experimental assessment; successfully injected animals were recovered and returned to group housing for a period of 5–6 weeks to allow for vector expression. New syringes and needles were used for each injection to avoid vector contamination between animals.

### Tissue harvesting

Five to 6 weeks postinjection, mice were killed by transcardial perfusion under terminal anesthesia; briefly, anesthetized mice were pinned in a supine position and the heart was visualized by removal of the rib cage. The right atrium was resected and 10 ml of phosphate-buffered saline (PBS) followed by 10 ml of formalin (10%, v/v) perfused into the left

ventricle. After perfusion all major organs (eyes, brain, lungs, heart, spleen, kidneys, liver, and pancreas) were harvested and trimmed of excess tissue. Once trimmed, half of each major organ system (e.g., one kidney) was cryoprotected in 30% sucrose overnight at 4°C before embedding in optimal cutting temperature (O.C.T.) medium, and the second half of each organ system was dehydrated for embedding in paraffin. O.C.T. blocks were stored at –80°C and paraffin blocks were stored at room temperature until sectioned.

### Histology

Paraffin slides (5 $\mu$m) for light microscopy were deparaffinized (xylene), rehydrated (graded ethanol washes), and subjected to citric acid epitope retrieval (Citra Solution; BioGenex, Fremont, CA) for 30 min before blocking with dual endogenous enzyme block (Dako, Carpinteria, CA) for 10 min. Nonspecific background staining was reduced further with Sniper (Biocare Medical, Walnut Creek, CA) for up to 60 min before sections were incubated with rabbit anti-GFP antibody (#ab290, 1:750 dilution; Abcam, Cambridge, MA) overnight at 4°C. GFP staining was visualized by MACH 2 rabbit–horseradish peroxidase (HRP) polymer detection (Biocare Medical) for 30 min and Liquid Permanent Red (Dako, Carpinteria, CA) administration. Slides were counterstained with hematoxylin (Biocare Medical) and mounted in Faramount aqueous medium (Dako). O.C.T. slides (12 $\mu$m) for fluorescence microscopy were permeabilized and subjected to autofluorescence eliminator reagent (Millipore) before being blocked with 10% normal donkey serum for 1 hr and incubated overnight with rabbit anti-GFP antibody (1:750 dilution; kind gift of W. Clay Smith, Department of Ophthalmology, University of Florida, Gainesville, FL) at 4°C. GFP staining to enhance native fluorescence was achieved with a fluorescein isothiocyanate (FITC)-conjugated donkey anti-rabbit antibody (1:350 dilution; Alexa Fluor 488; Invitrogen, Grand Island, NY) incubated for 1 hr at room temperature before counterstaining with Hoechst 33342 (1:500 dilution; Invitrogen) for 15 min and mounting with VECTASHIELD (Vector Laboratories, Peterborough, UK).

### Statistics

Two-way analysis of variance (ANOVA) with dilution and vector serotype as variables was used to assess the effect of AAV2 neutralizing antibodies on transduction efficiency. The effect of serotype on transduction efficiency was also assessed by one-way ANOVA with vector serotype as a variable; the Tukey or Sidak post-hoc test was applied as appropriate. Genome particle quantification between organs was assessed by two-tailed $t$ test. The significance set at $p < 0.05$ in all instances.

## RESULTS

The efficiency with which purified AAV vectors incorporating up to five Y–F/T–V mutations (TrplYF, TrplYF+TV, QuadYF, and QuadYF+TV; Fig. 1A) transduce endothelial cells was evaluated initially *in vitro*, using both primary endothelial cells harvested from bovine retinas and immortalized human umbilical vein endothelial cells (HUVECs). Purified vectors (Supplementary Table S1; supplementary data are available online at www.liebertpub.com/hum) packaging a ubiquitous promoter upstream of a fluorescent reporter gene (CBA-EGFP; Fig. 1B) were applied to primary bovine endothelial cells (MOI, $10^5$) and assessed 3 days later by fluorescence microscopy and flow cytometry, revealing that transduction efficacy increased proportionally to the number of amino acid substitutions (Fig. 1C–G). QuadYF+TV-mediated transduction was significantly higher than that achieved with unmodified rAAV2 capsid or capsid mutant variants containing fewer substitutions ($p < 0.0001$, all comparisons; one-way ANOVA with Tukey post-hoc test; Fig. 1H); this observation was additionally confirmed in HUVECs (Supplementary Fig. S1A–H).

On the basis of this initial observation, we evaluated the extent of endothelial transductions *in vivo* after systemic administration of the QuadYF+TV serotype vector. To this end, a luciferase (Luc) reporter construct was packaged into unmodified rAAV2 and QuadYF+TV serotype vectors (Supplementary Table S1); because of the large size of the luciferase reporter gene (1652 bp), a short variant (933 bp) of the endothelial cell-specific cadherin-5 promoter (smVECad) was used to drive expression (Fig. 2D). Purified vectors were injected intravenously into young adult (>8 weeks) nonpigmented mice (BALB/c) via the retro-orbital sinus, a venous drain located posterior of the eye at the orbit's medial wall.[32] Systemic expression was assessed by *in vivo* bioluminescence imaging 4 weeks after vector injection, revealing that intravenous administration of rAAV2.smVECad-Luc resulted in robust transduction of the liver (Fig. 2B). By contrast, QuadYF+TV.smVECad-Luc-injected animals demonstrated widespread bioluminescence signal throughout the abdomen, thorax, and head, with an apparent absence of liver transduction (Fig. 2C).

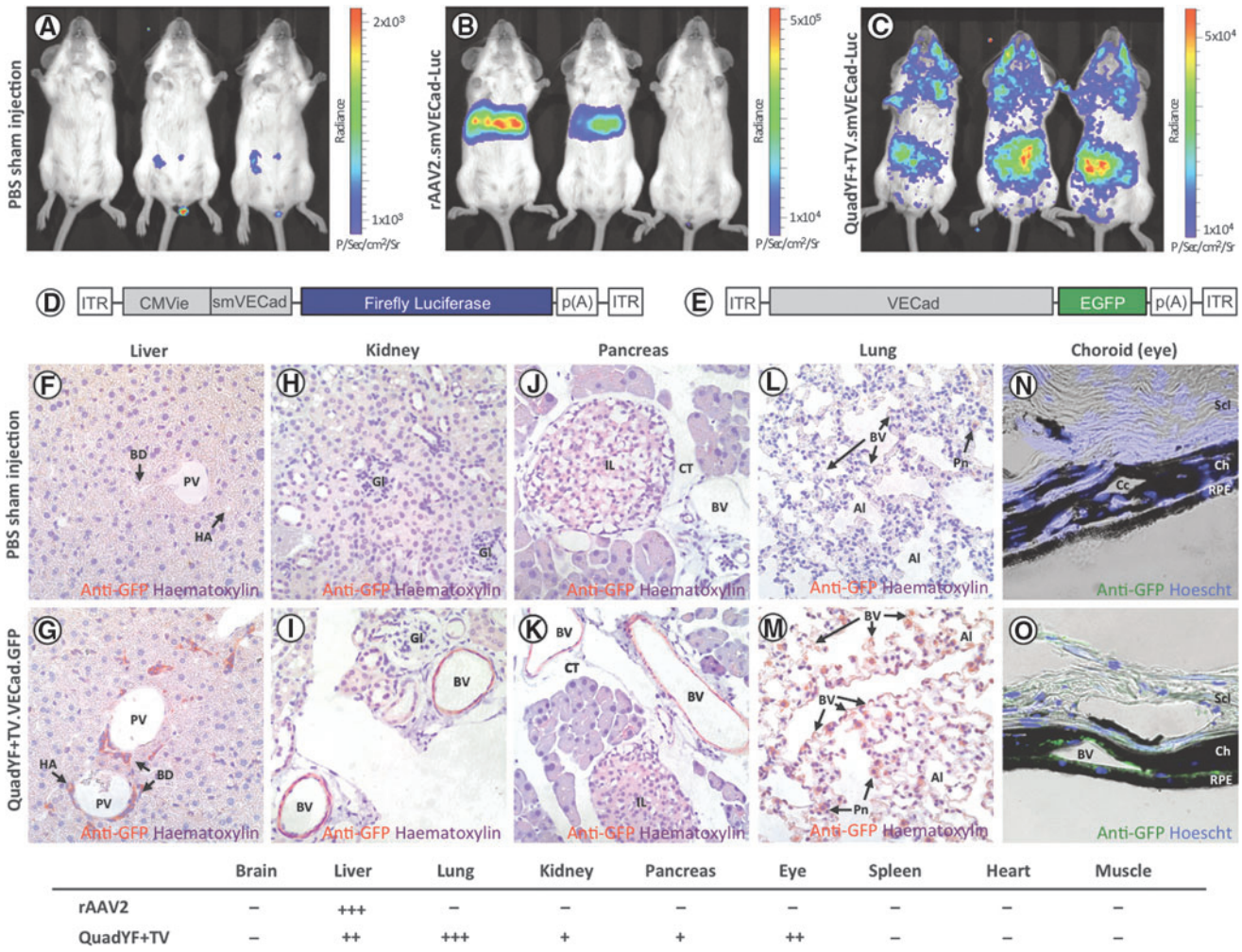


| | Brain | Liver | Lung | Kidney | Pancreas | Eye | Spleen | Heart | Muscle |
|---|---|---|---|---|---|---|---|---|---|
| rAAV2 | – | +++ | – | – | – | – | – | – | – |
| QuadYF+TV | – | ++ | +++ | + | + | ++ | – | – | – |

**Figure 2.** Bioluminescence imaging of BALB/cJ mice injected intravenously with either PBS **(A)**, unmodified AAV2 **(B)**, or QuadYF+TV **(C)** vector packaging an endothelial cell-specific luciferase reporter construct. **(D** and **E)** Schematic representation of the vectors used for *in vivo* assessment of tropism: **(D)** small vascular endothelial cadherin (smVECad) promoter and **(E)** full-length vascular endothelial cadherin (cadherin-5) promoter. Representative paraffin **(F–M)** or cryofrozen **(N** and **O)** sections of organs harvested from QuadYF+TV.VECad.GFP-injected mice versus PBS sham-injected controls (C57BL/6J; $n=9$ per group). Widespread transduction is observed in endothelial tissues of the liver **(F** and **G)**, kidney **(H** and **I)**, pancreas **(J** and **K)**, lung **(L** and **M),** and choroid of the eye **(N** and **O)**. Red signal **(F–M)**, anti-GFP immunostaining; green signal **(N** and **O)**, intrinsic fluorescence. *Bottom:* The relative levels of transduction across all injected animals ($n=9$) is summarized for each organ: –, no transduction observed in any animal; +, weak or inconsistent transduction observed; ++, moderate mostly consistent transduction observed; +++, strong very consistent transduction observed. AI, alveoli; BD, bile duct; BV, blood vessel; Ch, choroid; CT, connective tissue; HA, hepatic artery; GI, Glomeruli; IL, islet of Langerhans; Pn, pneumocyte; PV, portal vein; Scl, sclera; RPE, retinal pigment epithelium.

To assess tropism at the tissue level, young adult (>8 weeks) pigmented mice (C57BL/6J) were injected intravenously with unmodified rAAV2 vector or QuadYF+TV vector packaging a fluorescent reporter construct (enhanced green fluorescent protein; EGFP) under the control of either a ubiquitous or endothelial cell-specific promoter. In line with previous studies, extensive transduction of liver hepatocytes was observed after injection of either unmodified rAAV2 vector (data not shown) or QuadYF+TV vector packaging a ubiquitously expressing chicken $\beta$-actin (CBA) promoter (Fig. 3A and B). The inclusion of a full-length (2529 bp) endothelial cell-specific promoter (VECad) resulted in low-level liver transduction with substantially fewer hepatocytes transduced throughout; significantly, transgene expression within the liver was observed to be restricted predominantly to endothelial cells of the hepatic artery (HA), portal vein (PV), and bile ducts (BD) that comprise the portal triad (Fig. 2F and G, and Fig. 3C and D). Intravenous administration of QuadYF+TV.VECad-EGFP vector also resulted in limited transduction of several other organ systems, including the kidneys (Fig. 2H and I), pancreas (Fig. 2J and K), and eyes, where transduction was restricted predominantly to the blood vessels of the choroid (Fig. 2N and O), rather than the retinal vasculature (data not shown). In each organ, transduction was observed to be restricted primarily to the endothelium of the

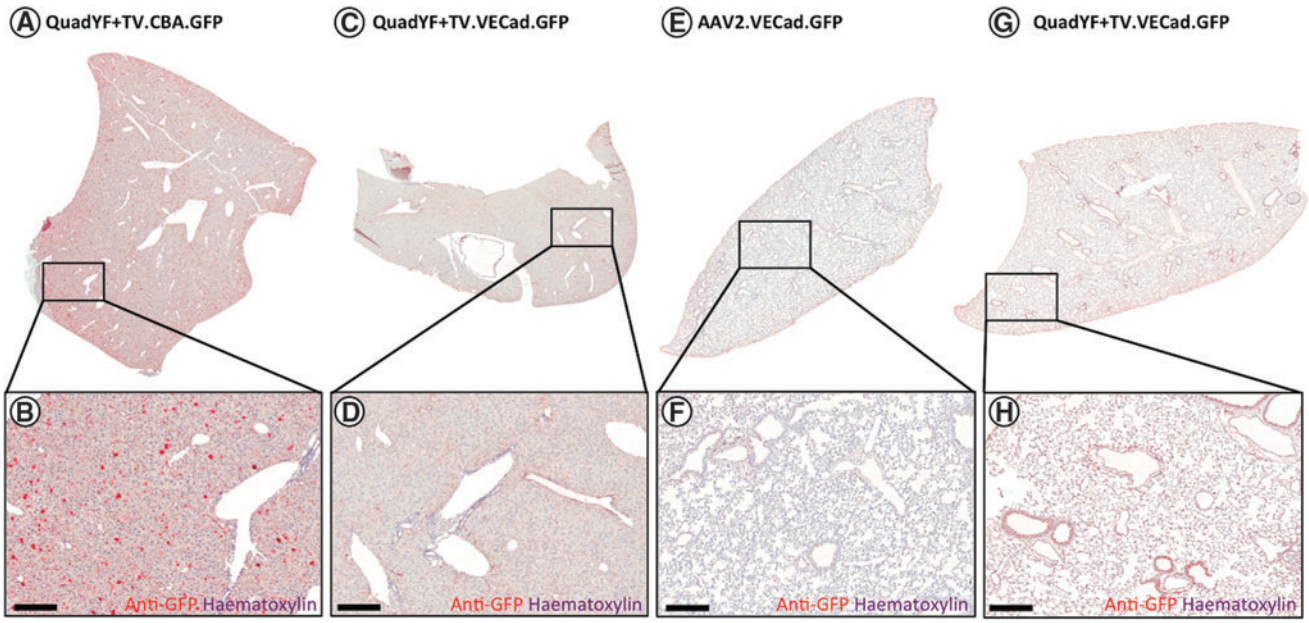


**Figure 3.** **(A–D)** Representative images of whole liver lobes from mice (C57BL/6) injected with QuadYF-TV packaging either a ubiquitously expressing chicken $\beta$-actin (CBA) promoter **(A** and **B)** or vascular endothelial cell-specific (VECad) promoter **(C** and **D)**, showing gross histological features; note the relative absence of hepatocyte transduction when using the endothelial cell-specific promoter. **(E–H)** Representative images of whole lung lobes harvested from unmodified rAAV2- and QuadYF-TV-injected mice (C57BL/6), showing gross histological features; note the relative absence of lung transduction in rAAV2-injected animals. Red signal **(A–H)**, anti-GFP immunostaining. Scale bars, 100 $\mu$m.

vasculature; no transgene expression was observed in the glomeruli (kidneys) or islets of Langerhans (pancreas). Strikingly, lungs harvested from QuadYF+TV.VECad-EGFP-injected animals demonstrated strong transgene expression throughout compared with rAAV2-injected animals with transduction of alveolar blood vessels and surrounding pneumocytes evident (Fig. 2L and M, and Fig. 3E–H). No transduction was observed in the heart, brain, spleen, or peripheral muscle (data not shown).

As it has previously been demonstrated that specific capsid mutations can lead to altered recognition by the humoral immune system,[33–36] we further evaluated the cross-reactivity of the QuadYF+TV vector with neutralizing antibodies raised against the wild-type AAV2 capsid, which are present in up to 30% of the human population.[37,38] rAAV2 and QuadYF+TV vectors packaging a ubiquitously expressing self-complementary fluorescent reporter construct (smCBA-mCherry; Fig. 4A) were preincubated with 2-fold dilutions (1:40, 1:80, 1:160, and 1:320) of primate serum containing either high (seropositive) or low (seronegative) levels of wild-type AAV2 neutralizing antibodies, as described previously (Fig. 4B).[24,31] The *in vitro* transduction efficiency of each vector was assessed on ARPE-19 cells by quantification of cellular fluorescence by flow cytometry after vector–serum coincubation. It was revealed that serum containing high levels of wild-type AAV2 neutralizing antibodies significantly inhibited transduction by QuadYF+TV at all dilutions compared with seronegative samples (Fig. 4C; $p < 0.0001$, all dilutions; two-way ANOVA with Sidak post-hoc test), indicating strong cross-reactivity even at low antibody concentrations.

## DISCUSSION

Herein, we have demonstrated that addition of up to five Y–F/T–V capsid mutations (Y272F, Y444F, T491V, Y500F, Y730F) increases vascular endothelial cell transduction in an additive manner, and critically leads to widespread transduction of the vasculature after intravenous administration. This finding strongly indicates that the QuadYF+TV capsid mutant vector may facilitate the targeted delivery of therapeutic transgenes to endothelial cells, allowing for the first time the possibility of treating long-term chronic vascular diseases after a single therapeutic intervention. In particular, the robust transduction of lung tissue observed is highly significant, indicating that the QuadYF+TV vector may be used for transgene delivery to tissues of the lung for the treatment of chronic diseases presenting with pulmonary complications, such as $\alpha_1$-antitrypsin

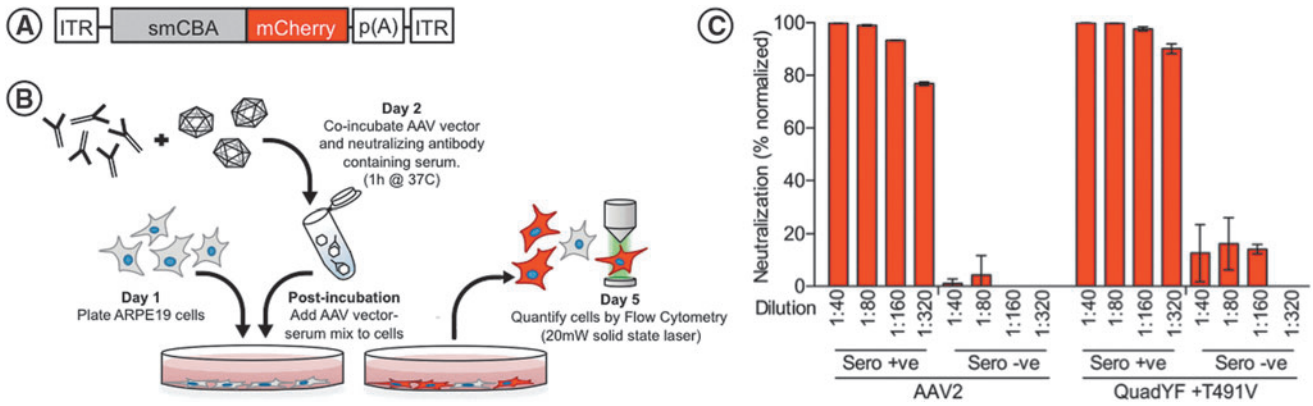


**Figure 4.** **(A)** Schematic representation of the self-complementary fluorescent reporter construct used for *in vitro* neutralization assay. ITR, inverted terminal repeat; smCBA, small chicken $\beta$-actin promoter; mCherry, red fluorescent reporter gene; p(A), polyadenylation signal. **(B)** Diagrammatic workflow of *in vitro* neutralization experiments. **(C)** Neutralization of AAV2 (*left*) and QuadYF-TV (*right*) vectors by serum containing high (Sero +ve) or low (Sero –ve) levels of neutralizing antibodies raised against AAV2 at dilutions ranging from 1:40 to 1:320 as assessed by flow cytometry. A high percentage of neutralization (90–100%) indicates that transduction of the ARPE-19 cells by the vector has been effectively inhibited, that is, little to no transgene expression was observed. It is clear that despite the introduction of five capsid mutations, circulating antibodies raised toward wild-type AAV2 recognize the QuadYF-TV vector capsid.

(ATT) deficiency. Although these findings are highly encouraging with respect to the potential treatment of human vascular disease, the extent and longevity of transgene expression in vascular endothelial cells would necessarily need to be assessed in relevant disease models, due to likely differences in transduction of abnormal (i.e., dysfunctional or angiogenic) vasculature and the rate of endothelial cell turnover, which is largely organ specific. In addition, there exist a number of factors that would likely complicate the clinical translatability of the QuadYF+TV vector if administered via a systemic approach.

First, the observation that circulating antibodies raised against wild-type AAV2 effectively neutralize the QuadYF+TV capsid would contraindicate use of the vector in many human patients, up to 30% of whom have preexisting immunity to wild-type AAV2. However, some studies have demonstrated that preexisting humoral immunity to the AAV capsid can be partly circumvented through treatment with "dummy" capsids that act to sequester circulating neutralizing antibodies.[39] Alternatively, preexisting immunity can be modulated through transient immunosuppression[40,41] or plasmapheresis,[33,42] although these have proven to be effective only in patients with low starting antibody titers.

Second, a substantial vector dose ($\sim 10^{12}$ vector genomes [VG] per animal) was required to achieve effective transduction efficiency in the mouse models used herein. An estimate based on blood volume and body mass relative to these study animals suggests that an effective dose for systemic administration in a human patient may be three to four orders of magnitude greater ($\sim 10^{15}$–$10^{16}$ VG) per patient. Although this would initially appear to be economically and logistically unfeasible, advances in AAV production technology based on packaging of rAAV using baculovirus or herpes simplex virus (HSV) platforms has led to significantly improved production capability for clinical-grade vector.[43–45]

Yet as a consequence of these barriers, the targeting of vascular endothelial cells from the luminal aspect may best be achieved through a combinative approach, using a vector with strong endothelial tropism (e.g., QuadYF+TV) administered via a targeted surgical delivery route. Specifically, this may be achieved through direct endovascular catheterization of the primary artery feeding a target organ. Such an approach has been used successfully to transduce liver hepatocytes in human patients with hemophilia after intrahepatic artery infusion of AAV-Factor IX.[34] By using a directed surgical approach to deliver vector to the vasculature of an individual organ, one would expect that the scope for vector neutralization would be substantially reduced because of delivery of virions in close proximity to the target endothelial cells. Furthermore, it is likely that this will lead to an increase in transduction efficiency, while simultaneously limiting the vector dose required per patient and the potential for ectopic gene expression. This last consideration may be particularly important when developing treatments aimed at preventing localized neovascularization through overexpression of antiangiogenic compounds (e.g., sFlt-1 for age-related macular degeneration) where off-target inhibition of angiogenesis—a normal

process in many tissues—may have serious deleterious effects. In more complex diseases, such as AAT deficiency, which affects multiple organ systems—notably the lungs and liver—it is unclear whether it would be beneficial to restrict expression of the therapeutic transgene (e.g., Serpina1) only to endothelial cells of the organ primarily affected (e.g., the lungs), dysfunction of which underlies the development of emphysema and is the primary cause of mortality in patients with AAT. Indeed, given the barriers to successful systemic administration, it may be beneficial in terms of maximizing therapeutic efficacy to treat each organ system individually, even in diseases that are systemic in nature (e.g., diabetes); this may be particularly relevant for the treatment of diseases where pathogenesis occurs at different rates in each organ system.

Although it was not possible to perform targeted intravenous cannulation in the rodent model presented herein, the injection route used (venous vs. arterial) may have contributed to the transduction pattern observed after QuadYF+TV vector administration. By administering vector into the venous branch via the retro-orbital venous sinus, one expects that the first major capillary bed to be encountered by AAV virions would be in the lungs—having first traversed the superior vena cava, heart, and pulmonary artery. The injection route chosen herein may account for the robust lung transduction observed, and supports previous evidence (e.g., see Ogura et al.[46] and Huda et al.[47]) that the site of vector delivery is critical to achieving effective transduction levels of a given target tissue. The relatively lower levels of transduction observed in other organs with the QuadYF+TV vector, despite its strong vascular tropism, is most likely associated with sequestration of virions by lymphoid tissues (e.g., the spleen) on reaching the arterial branch.[48]

In conclusion, we have described for the first time a capsid mutant AAV vector with strong tropism for vascular endothelial cells both *in vitro* and *in vivo*. The robust transduction of lung endothelial tissue after QuadYF+TV injection has particularly significant implications for the treatment of vascular disease with pulmonary etiology. The absence of endothelial transduction in the lungs of animals injected with unmodified rAAV2 vector via the same route (retro-orbital) highlights that a vector with strong endothelial cell-specific tropism is critical to achieving high levels of vascular transduction. However, that transduction of lung endothelial cells was observed to be strongest in QuadYF+TV-injected animals indicates that the route of administration may also be an important consideration to successfully achieving transduction of the endothelial cells of a specific organ. In human patients, systemic transgene expression may be problematic to achieve, or indeed undesirable, given the therapeutic transgene to be expressed. As a consequence, effective transduction of the vasculature may best be achieved by an approach that combines a vector demonstrating strong endothelial tropism with a surgical administration route intended to circumvent barriers to AAV transduction, such as endovascular catheterization.

## ACKNOWLEDGMENTS

Funding was contributed by the Juvenile Diabetes Research Foundation (JDRF; Innovative grant 1-PNF-20140120-A-N); by NIH grant P30EY021721; and by the Macular Vision Research Foundation, Foundation Fighting Blindness, Overstreet Fund, and Research to Prevent Blindness, Inc. D.M.L. was funded through a Fulbright-Fight for Sight UK Research Scholarship (#1396); S.E.B. was funded by the Foundation Fighting Blindness and by R01 EY024280. M.E.B. was funded by EY018358 and by a Research to Prevent Blindness unrestricted grant. The authors thank Dr. W. Clay Smith for providing the rabbit anti-GFP antibody and the Retinal Gene Therapy Vector Laboratory (University of Florida) for AAV vector production. Technical assistance from Jingfen Sun, Yuping Sun, and Zhonghong Zhang is also gratefully acknowledged. D.M.L. also acknowledges Dr. Bally for assistance during the preparation of this manuscript.

## AUTHOR CONTRIBUTIONS

D.M.L., S.L.B., and W.W.H. designed the study. D.M.L. carried out all *in vivo* experiments and led the study; C.A.R., S.E.B., X.Q., and M.E.B. contributed to *in vitro* experiments and histology; D.M.L. and J.J.P. carried out histology; D.M.L. performed data analysis and produced the figures; D.M.L. and W.W.H. wrote the manuscript with input from co-authors.

## AUTHOR DISCLOSURE

D.M.L., S.E.B., S.L.B., M.B., and W.W.H. currently have a provisional patent application (U.S. 62/116,863) relating to work presented herein. W.W.H. and the University of Florida have a financial interest in the use of AAV therapies, and own equity in a company (AGTC) that might, in the future, commercialize some aspects of this work.

## REFERENCES


1. Hamilton SJ, and Watts GF. Endothelial dysfunction in diabetes: pathogenesis, significance, and treatment. Rev Diabet Stud 2013;10:133–156.
2. Puddu P, Puddu GM, Zaca F, et al. Endothelial dysfunction in hypertension. Acta Cardiol 2000;55: 221–232.
3. Li H, Horke S, and Forstermann U. Vascular oxidative stress, nitric oxide and atherosclerosis. Atherosclerosis 2014;237:208–219.
4. Hadi HA, Carr CS, and Al Suwaidi J. Endothelial dysfunction: cardiovascular risk factors, therapy, and outcome. Vasc Health Risk Manag 2005;1: 183–198.
5. Tian XL, and Li Y. Endothelial cell senescence and age-related vascular diseases. J Genet Genomics 2014;41:485–495.
6. Schiffrin EL. Correction of remodeling and function of small arteries in human hypertension by cilazapril, an angiotensin I-converting enzyme inhibitor. J Cardiovasc Pharmacol 1996;27(Suppl 2):S13–S18.
7. Schiffrin EL, Park JB, Intengan HD, et al. Correction of arterial structure and endothelial dysfunction in human essential hypertension by the angiotensin receptor antagonist losartan. Circulation 2000;101:1653–1659.
8. Hornig B, Landmesser U, Kohler C, et al. Comparative effect of ace inhibition and angiotensin II type 1 receptor antagonism on bioavailability of nitric oxide in patients with coronary artery disease: role of superoxide dismutase. Circulation 2001;103:799–805.
9. Prasad A, Tupas-Habib T, Schenke WH, et al. Acute and chronic angiotensin-1 receptor antagonism reverses endothelial dysfunction in atherosclerosis. Circulation 2000;101:2349–2354.
10. McFarlane R, McCredie RJ, Bonney MA, et al. Angiotensin converting enzyme inhibition and arterial endothelial function in adults with type 1 diabetes mellitus. Diabet Med 1999;16:62–66.
11. Boger RH, Bode-Boger SM, Szuba A, et al. Asymmetric dimethylarginine (ADMA): a novel risk factor for endothelial dysfunction: its role in hypercholesterolemia. Circulation 1998;98:1842–1847.
12. Quyyumi AA, Dakak N, Diodati JG, et al. Effect of L-arginine on human coronary endothelium-dependent and physiologic vasodilation. J Am Coll Cardiol 1997;30:1220–1227.
13. Stroes E, Kastelein J, Cosentino F, et al. Tetrahydrobiopterin restores endothelial function in hypercholesterolemia. J Clin Invest 1997;99:41–46.
14. Heitzer T, Krohn K, Albers S, et al. Tetrahydrobiopterin improves endothelium-dependent vasodilation by increasing nitric oxide activity in patients with type II diabetes mellitus. Diabetologia 2000;43:1435–1438.
15. Higashi Y, Sasaki S, Nakagawa K, et al. Tetrahydrobiopterin enhances forearm vascular response to acetylcholine in both normotensive and hypertensive individuals. Am J Hypertens 2002;15:326–332.
16. Pistrosch F, Passauer J, Fischer S, et al. In type 2 diabetes, rosiglitazone therapy for insulin resistance ameliorates endothelial dysfunction independent of glucose control. Diabetes Care 2004;27:484–490.
17. Herweijer H, and Wolff JA. Progress and prospects: naked DNA gene transfer and therapy. Gene Ther 2003;10:453–458.
18. Bello A, Chand A, Aviles J, et al. Novel adeno-associated viruses derived from pig tissues transduce most major organs in mice. Sci Rep 2014;4:6644.
19. Chen S, Kapturczak M, Loiler SA, et al. Efficient transduction of vascular endothelial cells with recombinant adeno-associated virus serotype 1 and 5 vectors. Hum Gene Ther 2005;16:235–247.
20. Lu ZH, Kaliberov S, Zhang J, et al. The myeloid-binding peptide adenoviral vector enables multi-organ vascular endothelial gene targeting. Lab Invest 2014;94:881–892.
21. Nettelbeck DM, Miller DW, Jerome V, et al. Targeting of adenovirus to endothelial cells by a bispecific single-chain diabody directed against the adenovirus fiber knob domain and human endoglin (CD105). Mol Ther 2001;3:882–891.
22. Schiedner G, Bloch W, Hertel S, et al. A hemodynamic response to intravenous adenovirus vector particles is caused by systemic Kupffer cell-mediated activation of endothelial cells. Hum Gene Ther 2003;14:1631–1641.
23. Manickan E, Smith JS, Tian J, et al. Rapid Kupffer cell death after intravenous injection of adenovirus vectors. Mol Ther 2006;13:108–117.
24. Ryals RC, Boye SL, Dinculescu A, et al. Quantifying transduction efficiencies of unmodified and tyrosine capsid mutant AAV vectors *in vitro* using two ocular cell lines. Mol Vis 2011;17:1090–1102.
25. Petrs-Silva H, Dinculescu A, Li Q, et al. High-efficiency transduction of the mouse retina by tyrosine-mutant AAV serotype vectors. Mol Ther 2009;17:463–471.
26. Kay CN, Ryals RC, Aslanidi GV, et al. Targeting photoreceptors via intravitreal delivery using novel, capsid-mutated AAV vectors. PLoS One 2013; 8:e62097.
27. Iida A, Takino N, Miyauchi H, et al. Systemic delivery of tyrosine-mutant AAV vectors results in robust transduction of neurons in adult mice. Biomed Res Int 2013;2013:974819.
28. Qiao C, Zhang W, Yuan Z, et al. Adeno-associated virus serotype 6 capsid tyrosine-to-phenylalanine mutations improve gene transfer to skeletal muscle. Hum Gene Ther 2010;21:1343–1348.
29. Zolotukhin S, Byrne BJ, Mason E, et al. Recombinant adeno-associated virus purification using novel methods improves infectious titer and yield. Gene Ther 1999;6:973–985.
30. Cai J, Jiang WG, Grant MB, et al. Pigment epithelium-derived factor inhibits angiogenesis via regulated intracellular proteolysis of vascular endothelial growth factor receptor 1. J Biol Chem 2006;281:3604–3613.
31. Boye SE, Alexander JJ, Boye SL, et al. The human rhodopsin kinase promoter in an AAV5 vector confers rod- and cone-specific expression in the primate retina. Hum Gene Ther 2012;23:1101–1115.
32. Yamashita T, Takahashi A, and Honjin R. Spatial aspect of the mouse orbital venous sinus. Okajimas Folia Anat Jpn 1980;56:329–336.
33. Hurlbut GD, Ziegler RJ, Nietupski JB, et al. Preexisting immunity and low expression in primates highlight translational challenges for liver-directed AAV8-mediated gene therapy. Mol Ther 2010;18: 1983–1994.
34. Manno CS, Pierce GF, Arruda VR, et al. Successful transduction of liver in hemophilia by AAV-Factor IX and limitations imposed by the host immune response. Nat Med 2006;12:342–347.
35. Tseng YS, and Agbandje-McKenna M. Mapping the AAV capsid host antibody response toward the development of second generation gene delivery vectors. Front Immunol 2014;5:9.
36. Li C, Diprimio N, Bowles DE, et al. Single amino acid modification of adeno-associated virus capsid changes transduction and humoral immune profiles. J Virol 2012;86:7752–7759.
37. Moskalenko M, Chen L, van Roey M, et al. Epitope mapping of human anti-adeno-associated virus type 2 neutralizing antibodies: implications for gene therapy and virus structure. J Virol 2000;74: 1761–1766.
38. Halbert CL, Miller AD, McNamara S, et al. Prevalence of neutralizing antibodies against adeno-associated virus (AAV) types 2, 5, and 6 in cystic fibrosis and normal populations: implications for gene therapy using AAV vectors. Hum Gene Ther 2006;17:440–447.
39. Mingozzi F, Anguela XM, Pavani G, et al. Overcoming preexisting humoral immunity to AAV using capsid decoys. Sci Transl Med 2013;5: 194ra92.
40. Stasi R, and Provan D. Management of immune thrombocytopenic purpura in adults. Mayo Clin Proc 2004;79:504–522.
41. Mingozzi F, Chen Y, Edmonson SC, et al. Prevalence and pharmacological modulation of humoral immunity to AAV vectors in gene transfer to synovial tissue. Gene Ther 2013;20:417–424.
42. Monteilhet V, Saheb S, Boutin S, et al. A 10 patient case report on the impact of plasmaphe-

resis upon neutralizing factors against adeno-associated virus (AAV) types 1, 2, 6, and 8. Mol Ther 2011;19:2084–2091.

43. Smith RH, Levy JR, and Kotin RM. A simplified baculovirus–AAV expression vector system coupled with one-step affinity purification yields high-titer rAAV stocks from insect cells. Mol Ther 2009;17:1888–1896.

44. Clement N, Knop DR, and Byrne BJ. Large-scale adeno-associated viral vector production using a herpesvirus-based system enables manufacturing for clinical studies. Hum Gene Ther 2009;20:796–806.

45. Aslanidi G, Lamb K, and Zolotukhin S. An inducible system for highly efficient production of recombinant adeno-associated virus (rAAV) vectors in insect Sf9 cells. Proc Natl Acad Sci U S A 2009;106:5059–5064.

46. Ogura T, Mizukami H, Mimuro J, et al. Utility of intraperitoneal administration as a route of AAV serotype 5 vector-mediated neonatal gene transfer. J Gene Med 2006;8:990–997.

47. Huda F, Konno A, Matsuzaki Y, et al. Distinct transduction profiles in the CNS via three injection routes of AAV9 and the application to generation of a neurodegenerative mouse model. Mol Ther Methods Clin Dev 2014;1:14032.

48. Mori S, Takeuchi T, Enomoto Y, et al. Biodistribution of a low dose of intravenously administered AAV-2, 10, and 11 vectors to cynomolgus monkeys. Jpn J Infect Dis 2006;59:285–293.

Received for publication June 22, 2015;
accepted after revision August 15, 2015.

Published online: August 21, 2015.